Research article

The dynamics and harvesting strategies of a predator-prey system with Allee effect on prey

Chengchong Lu, Xinxin Liu* and Zhicheng Li

School of Data Science and Artificial Intelligence, Wenzhou University of Technology, Wenzhou, China

* **Correspondence:** Email: liuxx78@mail.sysu.edu.cn.

Abstract: The study of harvesting mechanisms in predator-prey systems with an Allee effect on prey has always garnered significant attention. In this paper, the dynamics and harvesting strategies of a predator-prey system are investigated, where the prey is subject to the Allee effect. The positivity and boundedness of solutions, the existence and stability of equilibria are further studied. The existence of a Hopf bifurcation at the interior equilibrium point of the system is investigated and verified by numerical simulations. Furthermore, we investigate the maximum sustainable yield (MSY), maximum sustainable total yield (MSTY) and the optimal economic profit of the proposed system. We find that MSY can be attained through predator harvesting, while MSTY is observed when harvesting efforts are uniform across species. In these situations, the biological system maintains stability. Using the method of control parametrization, the optimal economic profit and harvesting strategy are obtained. The results show that the harvesting efforts can affect the stability of the system, resulting in several interesting biological phenomena. This research provides a theoretical basis for biological resource management.

1. Introduction

The driving mechanism of predator-prey systems has consistently been a focal point in ecology, biomathematics and evolutionary biology [1–3]. The Allee effect in population ecology describes a phenomenon where a population's growth rate declines when its density falls below a specific threshold. The Allee effect was first proposed by an American ecologist called Allee in the early 20th century. In nature, many species have been reported to have the Allee effect, such as insects [4], plants [5], marine invertebrates [6], mammals [7] and so on. Many theoretical studies show that the

Allee effect has potential value in the study of small population dynamics [8–12], so it is more practical to consider the population model with the Allee effect. The Allee effect can be expressed in different forms in predator-prey systems:

(i) Population density threshold [13, 14]:

$$f(N) = \frac{bN}{A_1 + N},$$

where N is the density of the species, b is the highest per capita fertility of this species and A_1 is the Allee effect constant of this species. In population density threshold, when A_1 tends to 0, that is, under the influence of the weak Allee effect, we have $f = b$. When A_1 tends to infinity, that is, under the influence of the strong Allee effect, the population tends to go extinct more easily. The more significant the A_1, the stronger the Allee effect. When the population density is below a certain threshold, the survival and reproduction ability of the population will be affected.

(ii) Breeding threshold [15]:

$$f(N) = 1 - e^{-\varepsilon N},$$

where ε represents the Allee effect. When the population density is below a certain threshold, the reproduction rate of the population will decrease, resulting in the decrease of the population.

(iii) Pairing threshold [16–19]:

$$f(N) = \frac{N}{\mu + N},$$

where μ represents the Allee effect. When the population density is below a certain threshold, the pairing between individuals will be affected, resulting in a decrease in reproduction rate.

The Allee effect, described in these three expressions, has been thoroughly investigated. Wang et al. [20] studied the behavior of a reaction-diffusion predator-prey systems, with a strong Allee effect in the prey population. The authors demonstrated that the Allee effect significantly enhances the spatiotemporal complexity of the system. Hamada et al. [21] explored the influence of a weak Allee effect on the stability of a discrete-time predator-prey system, using mathematical analysis and numerical simulations. Rana et al. [22] explored a predator-prey system with Allee effects in both populations, conducting analyses for non-spatial and spatial models, and identifying conditions for instability and bifurcations. Zu and Mimura [23] studied the impact of the Allee effect on Rosenzweig-MacArthur predator-prey system with Holling type II functional response. The model is as follows:

$$\begin{cases} \dfrac{\mathrm{d}N}{\mathrm{d}t} = N\left(\dfrac{bN}{A_1 + N} - d_1 - \alpha N\right) - \dfrac{sNP}{1 + sh_1N}, \\ \dfrac{\mathrm{d}P}{\mathrm{d}t} = \dfrac{c_1 sNP}{1 + sh_1N} - d_2P, \end{cases} \tag{1.1}$$

where $N(t)$ is used to represent the density of the prey at time t and $P(t)$ is the density of the predator. Moreover, d_i are the per capita death rates of the prey and predator respectively, α denotes the strength of intra-competition of the prey, s denotes the effective search rate, h_1 denotes the handling time of the

predator, and c_1 denotes the conversion efficiency of the ingested prey into new predator. The authors found that the Allee effect of prey species increases the extinction risk of both predator and prey. Our model for this paper is based on this model.

In natural ecosystems, human interventions like harvesting can disrupt predator-prey systems. Therefore, it is crucial to consider the impact of harvesting effects when studying and managing these ecological dynamics. Dunne et al. [24] investigated the significant effects of food network structure in biodiversity loss, including secondary and 'cascade' extinctions. Ghosh et al. [25] considered an alternative harvesting function form to study MSTY and optimal tax policy. The harvesting function plays a crucial role in promoting system stability and preserving ecosystem equilibrium under specific conditions. Moreover, it enhances our ability to predict predator behavior. The most commonly used in a biological system is the proportional harvesting function [26–29], which is expressed as $H(x, E) = qEx$, where q represents the coefficient of harvesting and E is the harvesting effort.

The combined effects of harvesting and the Allee effect on the dynamics of predator-prey systems have gained increasing attention in both theoretical and empirical studies [30, 31]. Wu et al. [32] investigated the complex dynamical problems of a diffusive predator-prey system subject to strong Allee effects and threshold harvesting. They found that introducing strong Allee effects and harvesting efforts increased the spatiotemporal complexity of the system. Yu et al. [33] studied a Gauss predator-prey system with the Allee effect and Holling type III functional response and also considered the impact of predator competition and artificial fishing on predator-prey systems. They found that the model has multiple positive periodic solutions. Gupta and Yadav [34] researched a food-web model of these species in the presence of the multiplicative Allee effect and harvesting, and then observed that this makes the model more complex in the form of multiple coexisting steady states.

Studying harvesting items in predator-prey systems is crucial. Without considering harvesting efforts, our understanding remains limited, and real ecosystem dynamics are not accurately represented. Harvesting directly impacts predator and prey populations, shedding light on the true nature of these interactions. Additionally, it aids in validating and refining ecological models, underscoring the importance of investigating harvesting items. Hence, gaining insights into the impact of harvesting strategies on predator-prey dynamics, especially in the context of Allee effects, becomes imperative. Moreover, the linear harvesting function is often easier to analyze, making them invaluable for understanding the influence of harvesting in predator-prey systems with the Allee effect. Hence, this paper primarily focuses on an in-depth examination of the proportional harvesting function and the Allee effect.

Based on the previous studies and models, we add a harvesting function to the system (1.1), and finally, the predator-prey model is as follows:

$$
\begin{cases}
\dfrac{\mathrm{d}N}{\mathrm{d}t} = N\left(\dfrac{bN}{A_1 + N} - d_1 - \alpha N\right) - \dfrac{sNP}{1 + sh_1N} - q_1e_1N, \\
\dfrac{\mathrm{d}P}{\mathrm{d}t} = \dfrac{c_1sNP}{1 + sh_1N} - d_2P - q_2e_2P,
\end{cases}
\tag{1.2}
$$

where $e_i(i = 1, 2)$ are the harvesting efforts and $q_i(i = 1, 2)$ are the catch ability coefficients of the prey and predator, respectively. Due to biological considerations, $N(0) = N_0 > 0, P(0) = P_0 > 0$. To reduce variables and reduce operations, we perform the following transformation:

$$
N = \frac{\alpha x}{b}, P = \frac{sy}{b}, \tau = bt,
$$

for simplicity, we still use variabes x, y, t instead of N, P, τ. Then we obtain system (1.3)

$$\begin{cases} \dfrac{dx}{dt} = x\left(\dfrac{x}{A+x} - m_1 - x - \dfrac{y}{1+hx} - E_1\right) \triangleq f(x,y), \\ \dfrac{dy}{dt} = y\left(\dfrac{cx}{1+hx} - m_2 - E_2\right) \triangleq g(x,y), \end{cases} \tag{1.3}$$

where

$$A = \frac{A_1\alpha}{b}, m_1 = \frac{d_1}{b}, h = \frac{sh_1b}{\alpha}, m_2 = \frac{d_2}{b}, c = \frac{c_1s}{\alpha}, E_1 = q_1e_1, E_2 = q_2e_2,$$

where A is the recalculation intensity of the Allee effect, m_1 is the recalculation mortality of the prey, and m_2 is the recalculation mortality of the predator. $x(0) = x_0 > 0, y(0) = y_0 > 0$. All parameters are positive constants.

This paper is organized as follows. In section 2, we demonstrate the uniform boundedness of the system (1.3) in R_+^2. In section 3, we study the existence and stability of equilibrium points of the system. In section 4, we study the Hopf bifurcation of the system (1.3). In section 5, we give a comprehensive analysis of the harvesting strategy of the system (1.3), including MSY, MSTY and the optimal economic profit of the system (1.3). Conclusions are presented in section 6.

2. Positivity and boundedness

In this section, we demonstrate that the solutions of system (1.3) are positive and bounded using the techniques used in [35]. When the system satisfies positive initial conditions, it ensures the local existence and positivity of solutions, allowing both prey and predator populations to fluctuate within a defined range while remaining bounded.

Theorem 1. The solutions of the system (1.3) starting from $x_0 > 0, y_0 > 0$ are positive for all $t \geq 0$ and uniformly bounded.

Proof. From system (1.3), the solutions can be written as

$$\begin{aligned} x(t) &= x(0)e^{\int_0^t \left(\frac{x(s)}{A+x(s)} - m_1 - x(s) - \frac{y(s)}{1+hx(s)} - E_1\right)ds} > 0, \\ y(t) &= y(0)e^{\int_0^t \left(\frac{cx(s)}{1+hx(s)} - m_2 - E_2\right)ds} > 0, \end{aligned} \tag{2.1}$$

for all $t > 0$. Therefore, the solutions are positive.

Now we prove the boundedness of the system (1.3). Define the function

$$\Psi = x(t) + \frac{1}{c}y(t).$$

Integrating Ψ with respect to t, we get

$$\frac{d\Psi(t)}{dt} = \frac{dx}{dt} + \frac{1}{c}\frac{dy}{dt} = x\left(\frac{x}{A+x} - m_1 - x - E_1\right) - y\frac{m_2 + E_2}{c}.$$

Then

$$\frac{d\Psi}{dt} + (m_2 + E_2)\Psi = x\left(\frac{x}{A+x} - m_1 - x - E_1\right) + (m_2 + E_2)x$$

$$= -\left(x - \frac{m_2 + E_2 - m_1 - E_1}{2}\right)^2 + \frac{(m_2 + E_2 - m_1 - E_1)^2}{4}$$

$$\leq \frac{1}{4}(m_2 + E_2 - m_1 - E_1)^2 \triangleq W.$$

Applying the theory of differential inequality [36], we know that

$$0 < \Psi(t) \leq \frac{W}{m_2 + E_2}[1 - e^{-(m_2+E_2)t}] + \Psi(0)e^{-(m_2+E_2)t}.$$

As $t \to \infty$, we can see that the limit of the right-hand side is $W/(m_2 + E_2)$, so $\Psi(t)$ is bounded, and all solutions of the system (1.3) are bounded in the interior of R_+^2.

3. Existence and stability of equilibria

3.1. Existence of equilibria

The equilibria of the system are the intersection points of the prey isocline on which $\dot{x} = 0$ and the predator isocline on which $\dot{y} = 0$. We find that there are at most four equilibrium points in the system (1.3), which are one trivial equilibrium point (S_0), two axial equilibrium points (S_1, S_2) and one interior equilibrium point (S^*), where

$$S_0 = (0,0), S_1 = (x_1, 0), S_2 = (x_2, 0), S^* = (x^*, y^*). \tag{3.1}$$

Obviously, we can find that S_0 always exists. The form of $S_i(i = 1, 2)$ can be given from the following equation

$$x^2 - (1 - A - m_1 - E_1)x + A(m_1 + E_1) = 0, \tag{3.2}$$

where, if it exists, the form would be

$$x_i = \frac{1 - A - m_1 - E_1 \mp \sqrt{\Delta}}{2}(i = 1, 2), \tag{3.3}$$

where

$$\Delta = (1 - A - m_1 - E_1)^2 - 4A(m_1 + E_1). \tag{3.4}$$

We can easily prove that $x_i > 0$ if $\Delta > 0$; that is to say, $S_i(i = 1, 2)$ always exists if the following condition is satisfied

$$E_1 > A - m_1 + 2\sqrt{A} + 1 \quad \text{or} \quad E_1 < A - m_1 - 2\sqrt{A} + 1. \tag{3.5}$$

Then, we study the existence of the interior equilibrium point denoted by $S^*(x^*, y^*)$, where

$$x^* = \frac{m_2 + E_2}{c - m_2 h - E_2 h}, y^* = \left(\frac{x^*}{A + x^*} - m_1 - x^* - E_1\right)(1 + hx^*). \tag{3.6}$$

If S^* exists, the following conditions should be satisfied

$$E_2 < \frac{c - m_2 h}{h} \quad \text{and} \quad E_1 < \frac{m_2 + E_2}{Ac + m_2 + E_2 - Ahm_2 - AE_2 h} - m_1 - \frac{m_2 + E_2}{c - m_2 h - E_2 h}. \tag{3.7}$$

3.2. Stability of equilibria

The Jacobian matrix for the system (1.3) takes the following form

$$J_{(x,y)} = \begin{bmatrix} \frac{x(x+2A)}{(A+x)^2} - m_1 - 2x - \frac{y}{(1+hx)^2} - E_1 & -\frac{x}{1+hx} \\ \frac{cy}{(1+hx)^2} & \frac{cx}{1+hx} - m_2 - E_2 \end{bmatrix}.$$

3.2.1. Stability of $S_0(0,0)$

Theorem 2. S_0 is always locally asymptotically stable.

Proof. The Jacobian matrix about S_0 is given by

$$J_{S_0(0,0)} = \begin{bmatrix} -m_1 - E_1 & 0 \\ 0 & -m_2 - E_2 \end{bmatrix}.$$

It is easy to find that, at S_0, the Jacobian matrix J_{S_0} has two eigenvalues given by $\lambda_1 = -m_1 - E_1 < 0$ and $\lambda_2 = -m_2 - E_2 < 0$. We can know that S_0 is a locally asymptotically stable point, which indicates that when the density of the prey or predator lies in the attraction region of S_0, they will become extinct.

3.2.2. Stability of $S_i(x_i, 0)(i = 1, 2)$

The Jacobian matrix about $J_{S_i}(i = 1, 2)$ is given by

$$J_{S_i(x_i,0)} = \begin{bmatrix} \frac{Ax_i}{(A+x_i)^2} - x_i & -\frac{x_i}{1+hx_i} \\ 0 & \frac{cx_i}{1+hx_i} - m_2 - E_2 \end{bmatrix} (i = 1, 2).$$

The two eigenvalues are given by

$$\lambda_1 = \frac{Ax_i}{(A + x_i)^2} - x_i, \lambda_2 = \frac{cx_i}{1 + hx_i} - m_2 - E_2,$$

and we have proved that $\lambda_1 > 0$ at x_1 and $\lambda_1 < 0$ at x_2. Then, S_1 is a saddle point if $\lambda_2 < 0$, which is

$$E_2 > \frac{c(1 - A - m_1 - E_1 - \sqrt{\Delta})}{2 + h(1 - A - m_1 - E_1 - \sqrt{\Delta})} - m_2 \triangleq \eta_1, \tag{3.8}$$

and is a unstable point if $E_2 < \eta_1$.

S_2 is a saddle point if $\lambda_2 > 0$, which is

$$E_2 < \frac{c(1 - A - m_1 - E_1 + \sqrt{\Delta})}{2 + h(1 - A - m_1 - E_1 + \sqrt{\Delta})} - m_2 \triangleq \eta_2, \tag{3.9}$$

and is a stable point if $E_2 > \eta_2$. Then, we have the following theorem:

Theorem 3. (i) S_1 is a saddle point if $E_2 > \eta_1$, and is an unstable point if $0 < E_2 < \eta_1$.

(ii) S_2 is a stable point if $0 < E_2 < \eta_2$, and is a saddle point if $E_2 > \eta_2$.

3.2.3. Stability of $S^*(x^*, y^*)$

Theorem 4. S^* is locally asymptotically stable if $\varphi < 0$, and is unstable if $\varphi > 0$, where

$$\varphi = \frac{Ax^*}{(A + x^*)^2} + \frac{hx^*y^*}{(1 + hx^*)^2} - x^*.$$

Proof. The Jacobian matrix about S^* is given by

$$J_{S^*(x^*,y^*)} = \begin{bmatrix} \frac{x^*(x^*+2A)}{(A+x^*)^2} - m_1 - 2x^* - \frac{y^*}{(1+hx^*)^2} - E_1 & -\frac{x^*}{1+hx^*} \\ \frac{cy^*}{(1+hx^*)^2} & \frac{cx^*}{1+hx^*} - m_2 - E_2 \end{bmatrix} \triangleq \begin{bmatrix} a_{11} & a_{12} \\ a_{21} & a_{22} \end{bmatrix}.$$

The trace ($\mathrm{Tr}[J_{S^*}]$) and the determinant ($\mathrm{Det}[J_{S^*}]$) of Jacobian matrix J_{S^*} at S^* are given by

$$\mathrm{Tr}[J_{S^*}] = a_{11} + a_{22} = a_{11} = \frac{Ax^*}{(A + x^*)^2} + \frac{hx^*y^*}{(1 + hx^*)^2} - x^*,$$

$$\mathrm{Det}[J_{S^*}] = -a_{12}a_{21} = \frac{cx^*y^*}{(1 + hx^*)^3} > 0,$$

and the characteristic equation is given by $\lambda^2 - \mathrm{Tr}[J_{S^*}]\lambda + \mathrm{Det}[J_{S^*}] = 0$. Then, we have

$$\lambda_1 + \lambda_2 = \mathrm{Tr}[J_{S^*}], \lambda_1\lambda_2 = \mathrm{Det}[J_{S^*}].$$

Therefore, when $\mathrm{Tr}[J_{S^*}] < 0$, S^* is locally asymptotically stable, or it is unstable.

Theorem 5. Assume that S^* of the system (1.3) is locally asymptotically stable in R_+^2. Then, it is globally asymptotically stable if $E_1 > \max\left\{\frac{h(1-A)-1}{h} - m_1, \frac{1-A}{Ah+1} - m_1\right\}$.

Proof. Now we prove that there is no periodic orbit in R_+^2. Take a Dulac function

$$D(x, y) = \frac{(A + x)(1 + hx)}{xy},$$

and

$$R(x, y) = x\left(\frac{x}{A + x} - m_1 - x - \frac{y}{1 + hx} - E_1\right),$$

$$Q(x, y) = y\left(\frac{cx}{1 + hx} - m_2 - E_2\right),$$

then we have

$$\frac{\partial(D(x, y)R(x, y))}{\partial x} + \frac{\partial(D(x, y)Q(x, y))}{\partial y}$$

$$= -\frac{1}{y}\{3hx^2 + 2x[(m_1 + E_1)h + Ah + 1 - h] + (m_1 + E_1)(Ah + 1) + A + y - 1\},$$

which is negative in the first quadrant if the following condition holds:

$$E_1 > \max\left\{\frac{h(1 - A) - 1}{h} - m_1, \frac{1 - A}{Ah + 1} - m_1\right\}. \tag{3.10}$$

3.3. Numerical simulations

3.3.1. Existence and stability of equilibria

In this section, we perform numerical simulations to make analytical studies more complete. We take the parameters of the system (1.3) as

$$A = 0.003, m_1 = 0.19, m_2 = 0.07, h = 7, c = 3. \tag{3.11}$$

Based on analysis of the existence and stability of equilibrium points of the system (1.3), we give the partition diagram of the existence and stability of equilibria (see Figure 1).
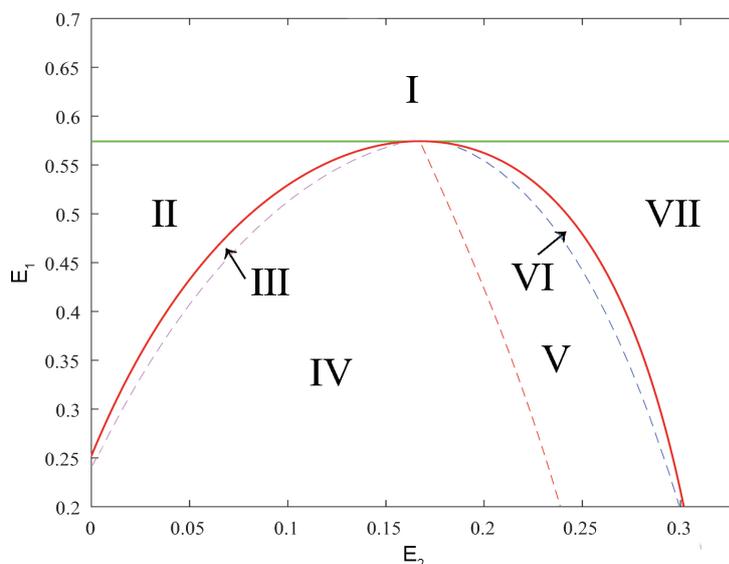

Figure 1. The partition diagram of the existence and stability of equilibria. Parameter values are given in (3.11).

We get that five lines ($l_i, i = 1, 2, 3, 4, 5$) divide the positive quadrant of the E_1E_2-plane into seven regions, named I-VII. The boundary between II and III, VI and VII is the line l_1, the boundary between III and IV is the line l_2, the boundary between IV and V is the line l_3, the boundary between V and VI is the line l_4 and the boundary between I and other regions is the line l_5, where

$$l_1 : E_1 = \frac{m_2 + E_2}{Ac + m_2 + E_2 - Ahm_2 - AE_2h} - m_1 - \frac{m_2 + E_2}{c - m_2h - E_2h},$$

$$l_2 : E_2 = \frac{c(1 - A - m_1 - E_1 - \sqrt{\Delta})}{2 + h(1 - A - m_1 - E_1 - \sqrt{\Delta})} - m_2,$$

$$l_3 : E_1 = \frac{x^*}{A + x^*} - m_1 - x^* - \left[1 - \frac{A}{(A + x^*)^2}\right](x^* + \frac{1}{h}),$$

$$l_4 : E_2 = \frac{c(1 - A - m_1 - E_1 + \sqrt{\Delta})}{2 + h(1 - A - m_1 - E_1 + \sqrt{\Delta})} - m_2,$$

$$l_5 : E_1 = A - m_1 - 2\sqrt{A} + 1.$$

The existence and stability of equilibrium points are shown in Table 1.

Then, we can give examples of each region (see Table 2). The corresponding solutions of the system in region I and region VI are presented in Figures 2 and 3.

Table 1. The existence of equilibrium points in the positive quadrant of the E_1E_2-plane.

partition		I	II	III	IV	V	VI	VII
	$S_0(0,0)$		exist					
Equilibrium point	$S_1(x_1,0)$		unstable		saddle point			
	$S_2(x_2,0)$	no exist	saddle point			stable		
	$S^*(x^*,y^*)$		no exist	unstable		stable		no exist

Table 2. The examples of each partition.

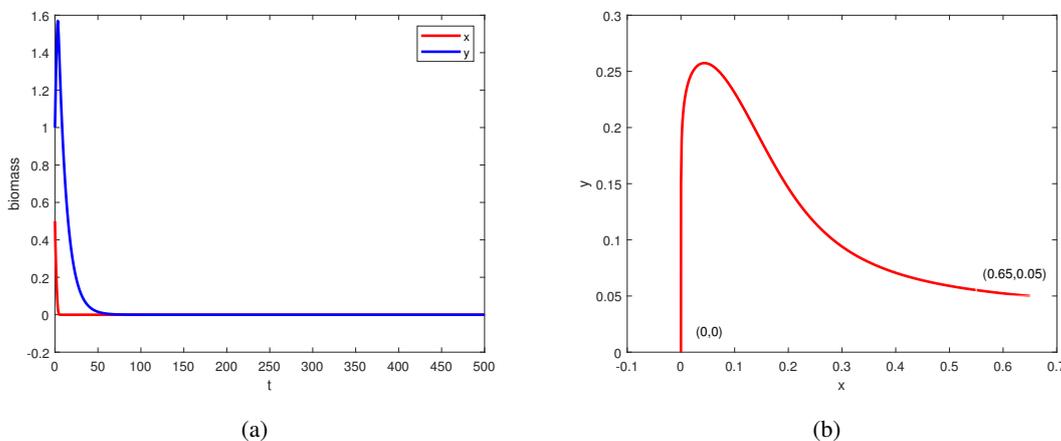|	E_1	E_2	Δ	S_0	S_1	S_2	S^*
I	0.65	0.05	$-0.0485 < 0$		no exist	no exist	no exist
II	0.5	0.05	$0.0586 > 0$		(0.0629,0)	(0.3051,0)	no exist
III	0.44523	0.055	$0.1089 > 0$		(0.0464,0)	(0.3764,0)	(0.0464,0.0000375)
IV	0.25	0.1	$0.3371 > 0$	exist	(0.0187,0)	(0.5993,0)	(0.0769,0.4297)
V	0.25	0.25	$0.3371 > 0$		(0.0187,0)	(0.5993,0)	(0.3333,0.7636)
VI	0.4724	0.2523	$0.0832 > 0$		(0.0536,0)	(0.342,0)	(0.341,0.0001123)
VII	0.45	0.3	$0.1043 > 0$		(0.0475,0)	(0.3705,0)	no exist

(a)

(b)

Figure 2. (a) Paths of the prey and predator species. (b) The phase plane trajectories. $(E_1, E_2) = (0.65, 0.05)$, the other parameter values are given in (3.11).
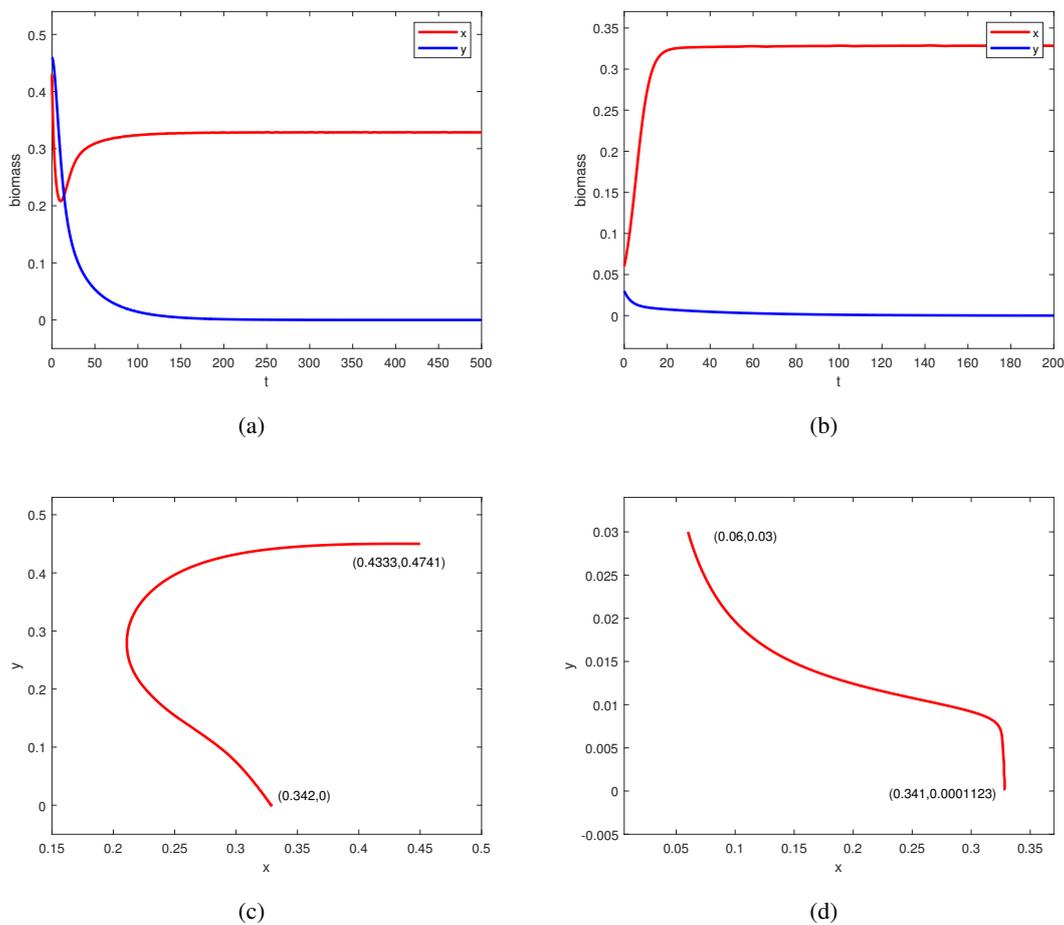
Figure 3. (a)(b): Paths of the prey and predator species under different initial values. (c)(d): The phase plane trajectories under different initial values. The initial values of (a)(c) is (0.4333,0.4741) and the initial values of (a)(c) is (0.06,0.03). $(E_1, E_2) = (0.4724, 0.2523)$, the other parameter values are given in (3.11).

Through the analysis and simulations of equilibrium points in region VI, we have identified two stable equilibrium points. The system's stability depends on the initial population densities. Under the combined influence of the Allee and harvesting effects, when the initial population densities of both species are high, the predator population faces extinction. Conversely, when the initial densities are low, coexistence of the predator and prey populations is possible.

In terms of biology, coexistence is observed with harvesting efforts in regions V and VI, but both species go extinct when efforts are in region I. This highlights the importance of controlling harvesting intensity to maintain the coexistence of both prey and predator populations.

3.3.2. The impact of the harvesting

In the following, we study the effect of the harvesting effect on the predator-prey systems. Under the same parameter values given in (3.11) and the same initial conditions as Figure 3, the paths of the prey and predator species of system (1.1) are given in Figure 4.
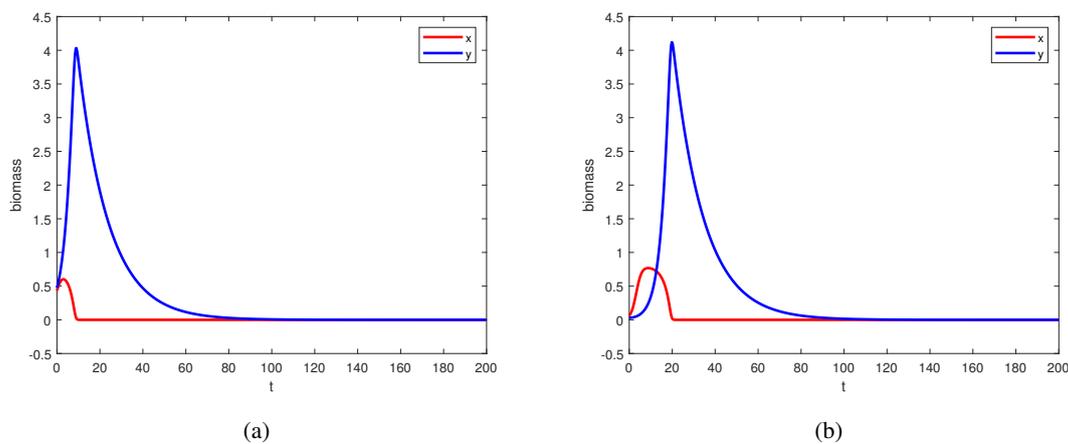
Figure 4. Paths of the prey and predator species. (a) (x_0, y_0)=$(0.4333, 0.4741)$. (b) (x_0, y_0)=$(0.06, 0.03)$. $(E_1, E_2) = (0.4724, 0.2523)$. The relevant parameter values are given in (3.11).

.

Simulation results indicate that populations in system (1.1) tend towards $(0, 0)$, indicating the extinction of both prey and predator. Without the influence of harvesting efforts, the system remains unstable, and predator-prey coexistence is unattainable regardless of initial population densities. Comparing system (1.1) to system (1.3), we observe that low-density populations, which could not coexist, achieve coexistence under the influence of harvesting. Conversely, at high population densities, the prey, which could not survive, persists due to harvesting efforts, while the predator goes extinct.

Limit cycles represent periodic fluctuations in population numbers over time within a system. In real-world ecological systems, these periodic fluctuations play a critical role in establishing a dynamical equilibrium between prey and predator, preventing the unchecked growth or extinction of populations. We can numerically simulate the limit cycles of the system by choosing the following parameters

$$A = 0.003, m_1 = 0.19, m_2 = 0.07, h = 7, c = 3, E_1 = 0.4, E_2 = 0.13. \tag{3.12}$$

In this case, $S^*(0.1452, 0.6746)$ is unstable, and a limit cycle appears in the system (1.3) with periodic behavior. This is shown in Figure 5.

In order to further study the effect of the harvesting items on the system, we investigate the sensitivity of predator populations in system (1.1) and system (1.3) to parameters (Figure 6). In the process of controlling variables, the parameters are given as

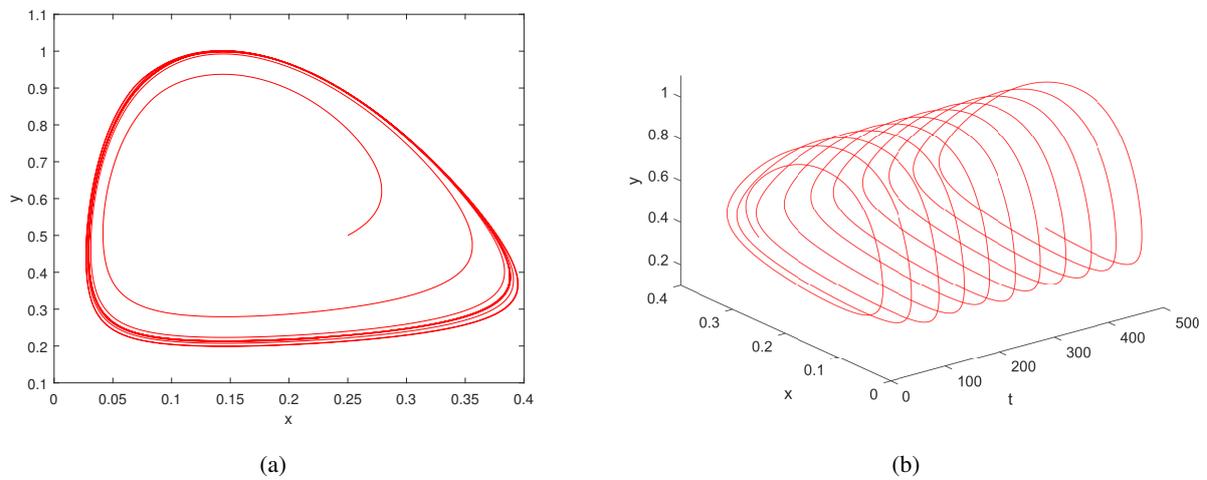$$m_1 = 0.1, m_2 = 0.05, h = 4, c = 4.8, A = 0.04, E_1 = 0.3, E_2 = 0.6. \tag{3.13}$$

Figure 5. (a) The phase diagram of the limit cycle. (b)The paths with time of x and y. The relevant parameter values are given in (3.12).
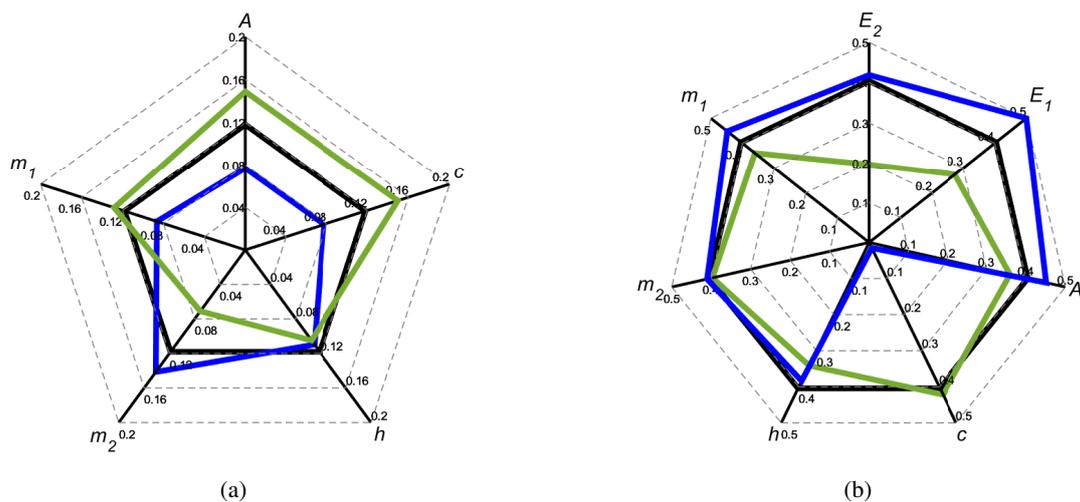

Figure 6. (a) The influence of different parameters on predator population without harvesting effect. (b) The influence of different parameters on predator population under harvesting effect.

We investigate dynamic changes in the predator population by altering parameters in the prey-predator dynamics. In Figure 6, the blue line illustrates equilibrium point changes as each variable increases by 20%, while the green line shows changes when each variable decreases by 20%, with the original values represented by the black line. Without harvesting, variables A, c, m_1 and m_2 exert a substantial influence on the predator population. A 20% increase in A, c, h and m_1 leads to a decrease in predator numbers, while an increase in m_2 results in higher predator numbers. The decline in m_2 is attributed to a significant decrease in the predator population. Under the influence of harvesting, variables c, E_1 and E_2 have a pronounced impact on predator numbers. An increase in c negatively affects predator populations, posing a threat to their existence. The presence of harvesting

efforts (E_1, E_2) mitigates the influence of the Allee effect. Notably, the number of predators varies with the level of harvesting effort. An increase in conversion rate c can significantly disrupt ecosystem stability, potentially disturbing the ecological balance.

3.3.3. The impact of the Allee effect

In system (1.1), it becomes evident that when the interior equilibrium point is unstable, the Allee effect on the prey species is more pronounced. Conversely, when the interior equilibrium point is stable, the Allee effect on the prey species has a weaker influence. Furthermore, as the intensity of the Allee effect increases, the region of stable coexistence between predator and prey contracts. The coexistence of prey and predator populations hinges on their initial placement within this stable region; otherwise, they risk extinction.

To further investigate the influence of the Allee effect on the system, we vary its strength using two different values of A, specifically 0.003 and 0.1. Then we conduct numerical simulations utilizing parameter (3.11), as depicted in Figure 7.
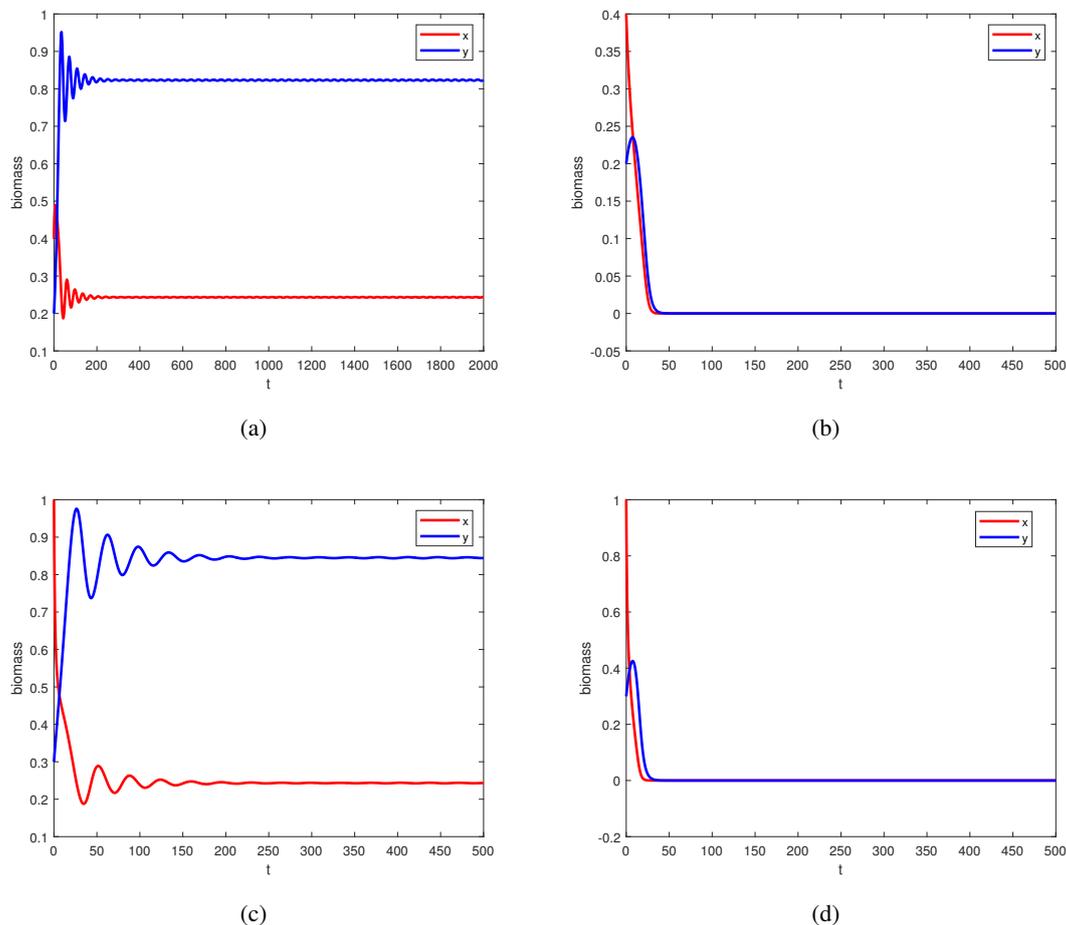

(a)

(b)

(c)

(d)

Figure 7. Paths of the prey and predator species. The initial values of (a)(b) are $(x_0, y_0)=(0.4, 0.2)$. The initial values of (c)(d) are $(x_0, y_0)=(1, 0.3)$. The A values of (a)(c) are 0.003. The A values of (b)(d) are 0.1, the other parameter values are given in (3.11)
.

In the system (1.3), the coexistence of predator and prey is contingent upon the stability of the interior equilibrium point; otherwise, both populations may face extinction. In essence, when the Allee effect is particularly strong, prey populations tend to decrease over time, elevating the risk of extinction. However, an intriguing phenomenon arises when the initial populations of predators and prey differ significantly: the predator population gradually overtakes that of the prey, eventually resulting in a state of coexistence.

4. Hopf bifurcation

In nature, under the influence of human interference-harvesting, the predator-prey systems tends to produce oscillatory behavior and may also have limited cycles. Due to a cyclic nature, the populations in the system may exhibit periodic fluctuations, periodic crashes, or outbreak events. The Hopf bifurcation marks the transition from a stable state to a periodic oscillation state, which is of great significance to the long-term stability of an ecosystem. By controlling the intensity of harvest, we can avoid such crashes and then maintain the stable survival of the population system. In the following, we will analyze Hopf bifurcation. Through the preceding analysis, S^* may lose its stability through Hopf bifurcation under certain parameter restrictions. Consider E_2 as the bifurcation parameter. Then, according to the definition of Hopf birfucation, we have $\mathrm{Tr}[J_{S^*}] = 0$ and $\mathrm{Det}[J_{S^*}] > 0$. Then, from

$$\mathrm{Tr}[J_{S^*}] = a_{11} = \frac{Ax^*}{(A+x^*)^2} - x^* + \frac{hx^*y^*}{(1+hx^*)^2} = 0,$$
$$\mathrm{Det}[J_{S^*}] = \frac{cx^*y^*}{(1+hx^*)^3} > 0.$$

We draw that the bifurcation threshold is a positive root of $\mathrm{Tr}[J_{S^*}] = 0$ and the bifurcation parameter is given by $E_2 = E_2^H$, which satisfies $\mathrm{Det}[J_{S^*}]\big|_{E_2=E_2^H} > 0$.

Assume that the parameters satisfy the conditions for the existence of equilibrium point S^*. Then S^* changes its stablity through Hopf bifurcation threshold $E_2 \equiv E_2^H$ such that $\mathrm{Tr}[J_{s^*}]\big|_{E_2=E_2^H} = 0$. Obviously, at $E_2 = E_2^H$, let $\omega^2(E_2^H)$ denote $\mathrm{Det}(E_2^H)$ and S^* have eigenvalues $\lambda_{1,2}(E_2^H) = \pm i\omega(E_2^H)$. We use the normal form theorem [36] for analysis. We get that

$$\frac{\mathrm{d}}{\mathrm{d}E_2}\mathrm{Tr}[J_{S^*}]\bigg|_{E_2=E_2^H} = \frac{2}{g_1} - \frac{2(m_2+E_2)(Ah-1)}{g_2^2} - \frac{h(2E_2+2m_2)}{g_1^2} +$$
$$\frac{(Ah-1)[h(E_2+m_2)^2 - 2Ag_1(c+E_2h+hm_2)]}{hg_2^3}\bigg|_{E_2=E_2^H} \neq 0,$$

where $g_1 = E_2h - c + hm_2$, $g_2 = E_2 + m_2 + Ac - AE_2h - Ahm_2$.

Then, we compute the first Lyapunov coefficient [37]. Fixing the parameter E_2 at its critical value E_2^H, S^* at $E_2 = E_2^H$ has the coordinates $\left(x_1^H\big|_{E_2=E_2^H}, y_1^H\big|_{E_2=E_2^H}\right)$. Translating the origin of the coordinates at this equilibrium point by the change of variables

$$\begin{cases} x = x_h + x_1^H\big|_{E_2=E_2^H}, \\ y = y_h + y_1^H\big|_{E_2=E_2^H}, \end{cases}$$

and then expanding in Taylor series, we have

$$
\begin{cases}
\dot{x}_h = \mu_{10}x_h + \mu_{01}y_h + \mu_{20}x_h^2 + \mu_{11}x_hy_h + \mu_{02}y_h^2 + \mu_{30}x_h^3 \\
\qquad + \mu_{21}x_h^2y_h + \mu_{12}x_hy_h^2 + \mu_{03}y_h^3 + W(x_h, y_h), \\
\dot{y}_h = v_{10}x_h + v_{01}y_h + v_{20}x_h^2 + v_{11}x_hy_h + v_{02}y_h^2 + v_{30}x_h^3 \\
\qquad + v_{21}x_h^2y_h + v_{12}x_hy_h^2 + v_{03}y_h^3 + T(x_h, y_h),
\end{cases}
$$

where $\mu_{10}, \mu_{01}, v_{10}, v_{01}$ are the elements of Jacobian matrix evaluated at the equilibrium point S^* and $E_2 = E_2^H$. Since we have

$$
\mu_{10} + v_{01} = 0,
$$
$$
\Delta = \mu_{10}v_{01} - \mu_{01}v_{10} > 0.
$$

The coefficients μ_{ij} and v_{ij} are determined by

$$
\mu_{10} = \frac{x_h(x_h + 2A)}{(A + x_h)^2} - m_1 - 2x_h - \frac{y_h}{(1 + hx_h)^2} - E_1, \quad \mu_{01} = -\frac{x_h}{1 + hx_h},
$$
$$
\mu_{20} = \frac{1}{x_h + A} - \frac{x_h^2 + 2Ax_h}{(x_h + h)^3} + \frac{y_hh}{(1 + hx_h)^3} - 1, \quad \mu_{11} = -\frac{1}{(1 + hx_h)^2},
$$
$$
\mu_{30} = -\frac{1}{(x_h + A)^2} + \frac{x_h^2 + 2Ax_h}{(x_h + A)^4} - \frac{y_hh^2}{(1 + hx_h)^4}, \quad \mu_{21} = \frac{h}{2(1 + hx_h)^3},
$$
$$
\mu_{02} = \mu_{12} = \mu_{03} = 0,
$$

and

$$
v_{10} = \frac{cy_h}{(1 + hx_h)^2}, \quad v_{20} = -\frac{cy_hh}{(1 + hx_h)^3}, \quad v_{11} = \frac{c}{(1 + hx_h)^2},
$$
$$
v_{30} = \frac{cy_hh^2}{2(1 + hx_h)^4}, \quad v_{21} = -\frac{ch}{(1 + hx_h)^3}, \quad v_{01} = \frac{cx_h}{1 + hx_h} - m_2 - E_2,
$$
$$
v_{02} = v_{12} = v_{03} = 0,
$$

and $W(x_h, y_h)$ and $T(x_h, y_h)$ are power series in (x_h, y_h) with terms $x_h^iy_h^j$ satisfying $i + j \geq 4$.

The first Lyapunov number l_1 [38], which is used to determine the stability of limit cycle around the Hopf bifurcation, is given by

$$
\begin{aligned}
l_1 = &\frac{-3\pi}{2\mu_{01}\Delta^{\frac{3}{2}}}\{[\mu_{10}\mu_{01}(v_{11}^2 - 2\mu_{20}^2 + \mu_{20}v_{11} + 2v_{20}v_{02} + \mu_{11}v_{02}) \\
&+ \mu_{10}v_{10}(\mu_{11}^2 - 2v_{02}^2 + \mu_{11}v_{02} + 2\mu_{20}\mu_{02} + \mu_{02}v_{11}) + \mu_{01}v_{10}(v_{11}v_{02} - \mu_{11}\mu_{20})] \\
&+ v_{10}^2(2\mu_{02}v_{02} + \mu_{11}\mu_{02}) - 2\mu_{10}^2v_{11}v_{02} + 2\mu_{10}^2\mu_{11}\mu_{20} - \mu_{01}^2(2\mu_{20}v_{20} + v_{11}v_{20}) \\
&- (\mu_{10}^2 + \mu_{01}v_{10})[v_{10}\mu_{12} - \mu_{01}v_{21} + 2\mu_{10}(v_{12} + \mu_{21}) + 3(v_{03}v_{01} - \mu_{30}\mu_{01})]\}.
\end{aligned}
$$

Furthermore, the first Lyapunov number in system (1.3) is given by the following form

$$
\begin{aligned}
l_1 = &\frac{3\pi}{2x_h\Gamma^{\frac{3}{2}}}\Big\{(a_2^2 - a_4)\Big[\frac{3x_hy_h(-a^2 + ab^2 + 4abx_h + 6ax_h^2 - x_h^4)}{a_5^5} + \frac{\mu x_ha_1}{a_5^4} + \frac{2a_2a_1}{a_5^3}\Big] \\
&+ \frac{x_h^2[2\mu y_ha_3a_1a_5^2 + \mu^2y_h(-x_h^2 + a)a_1]}{a_5^7} - \frac{\mu y_ha_2(a - x_h^2)^3}{a_5^6} - \frac{2x_ha_3^2a_2}{a_5}
\end{aligned}
$$

$$+ \frac{a_2 x_h[\mu^2(a - x_h^2)^2 + \mu a_3 a_5^2(a - x_h^2)]}{a_5^5} - \frac{a_3(2a_2^2 + a_4)(a - x_h^2)}{a_5^2} \Bigg\},$$

where

$$a_1 = (hx_h + 1)^4, a_2 = m_1 + E_1 + 2x_h + \frac{y_h}{a_5} - \frac{a_6}{(A + x_h)^2}, a_3 = \frac{1}{A + x_h} - \frac{a_6}{(A + x_h)^3} + \frac{hy_h}{a_7} - 1,$$

$$a_4 = \frac{cx_h y_h}{a_7}, a_5 = (hx_h + 1)^2, a_6 = x_h(2A + x_h), a_7 = (hx_h + 1)^3.$$

If $l_1 < 0$, the Hopf bifurcation is supercritical, which means that S^H would lose stability. If $l_1 > 0$, the Hopf bifurcation is subcritical.
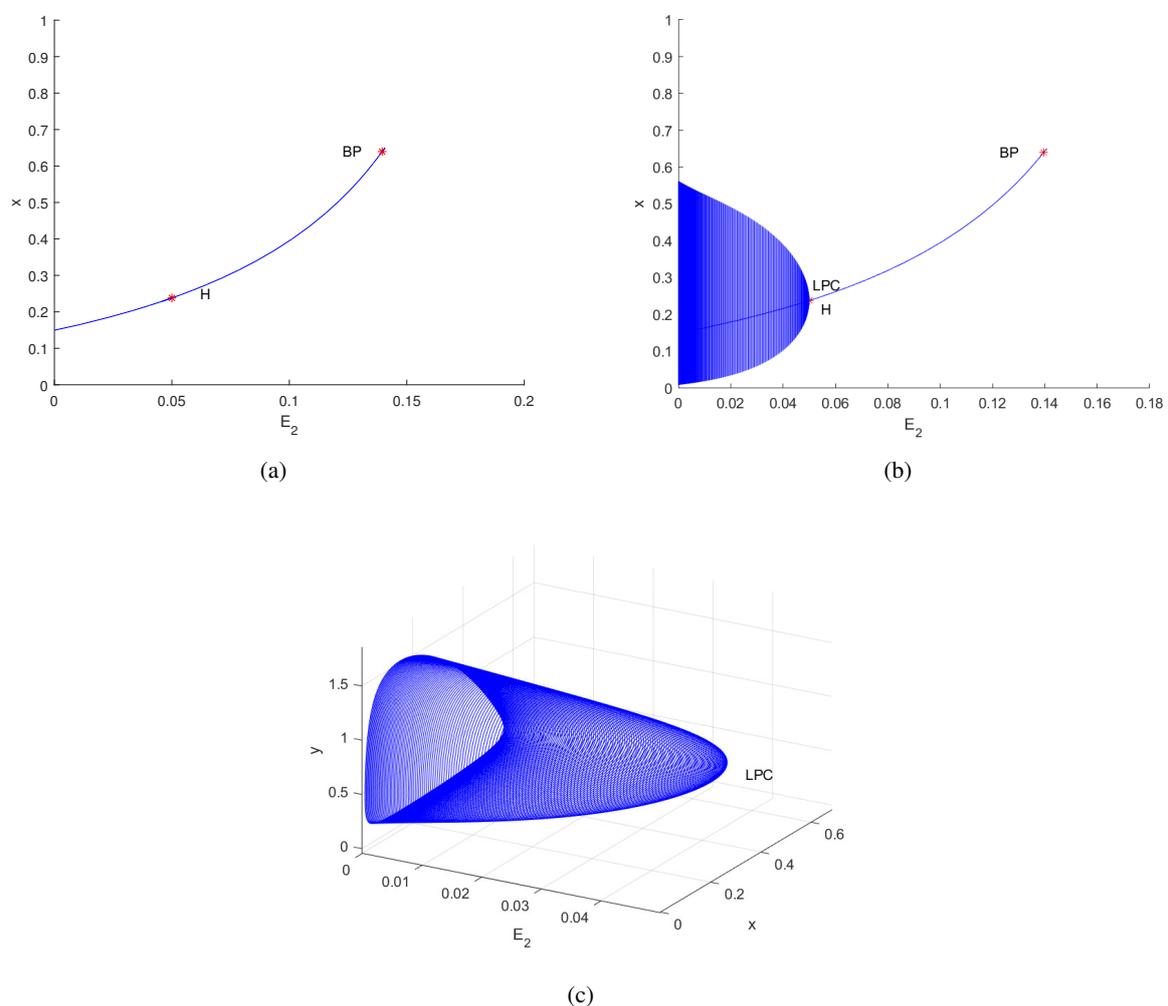

(a)

(b)

(c)

Figure 8. (a) Equilibrium bifurcation diagram. (b) Continuation of S^* equilibrium curve for bifurcation parameter E_2. (c) Continuation of the limit cycle. The parameters are given in (4.1).

Next, we analyze the Hopf bifurcation curve via the MATLAB toolbox matcont. Take the following parameters

$$m_1 = 0.1, m_2 = 0.2, h = 5.8, c = 2.5, E_1 = 0.2573, A = 0.002. \tag{4.1}$$

Then, we can find that the following equation (4.2) satisfies the transversal condition of Hopf bifurcation

$$\frac{\mathrm{d}}{\mathrm{d}E_2}\mathrm{Tr}[J_{S^*}]\bigg|_{E_2=E_2^H} = -11.3 \neq 0.$$

The Hopf bifurcation threshold for E_2^* is 0.050001754. In the MATLAB Command Window, there is a bifurcation point detected: a Hopf point (labeled by H) around $S^*(0.238099, 0.943511)$ (Figure 8 (a)(b)). The first Lyapunov coefficient is -0.4663762. In this occasion, the Hopf bifurcation is supercritical, and a stable limit cycle may bifurcate there, which means that when the population sizes reach specific values, they fluctuate around them without infinitely increasing or decreasing. This periodic regulation helps maintain relatively balanced population sizes and prevents one population from growing or declining indefinitely. Further, we give the phase portraits of the limit cycle to observe the change of limit cycle with bifurcation parameters (Figure 8 (c)).

5. Harvesting strategy research

5.1. Yield analysis

Yield analysis is one of the key methods to study the sustainable utilization of resources in predator-prey systems. The maximum sustainable yield (MSY) is the maximum fishery output that humans can get on the basis of protecting the ecological environment. Under the premise of ensuring the sustainable survival of all populations in the system, harvesting all populations and achieving the maximum yield is called the maximum sustainable total yield (MSTY) [39, 40]. First, we investigate if, for system (1.3), MSTY exists. The yield function at S^* is

$$Y(E_1, E_2) = -E_2(1 + hx)\left(m_1 + E_1 + x - \frac{m_2 + E_2}{m_2 + E_2 + Ac - Ahm_2 - AhE_2}\right) - \frac{E_1(m_2 + E_2)}{hm_2 + hE_2 - c}.$$

If MSTY exists, the optimal harvesting efforts E_1 and E_2 are the solution of $\partial Y/\partial E_1 = 0$ and $\partial Y/\partial E_2 = 0$ and the Hessian matrix is negative definite. The Hessian matrix of Y is

$$H = \begin{bmatrix} 0 & \frac{\partial^2 Y}{\partial E_1 \partial E_2} \\ \frac{\partial^2 Y}{\partial E_2 \partial E_1} & \frac{\partial^2 Y}{\partial E_2^2} \end{bmatrix}.$$

We know that the H matrix is negative definite if, and only if, the odd-order orderings of H are all less than 0 and the even-order orderings of H are all greater than 0. Because Y is linear with respect to E_1, and $\triangle_1 = \partial^2 Y/\partial E_1^2 = 0$, the sufficient condition for Y to maximize (E_1, E_2) is not satisfied.

In the following, we will discuss whether there is MSTY of the system when the harvesting effort on the prey and the predator is the same. The yield function of the equilibrium state is

$$W(E) = -E(1 + hx)\left[m_1 + E + x - \frac{m_2 + E}{(m_2 + E)(1 - AH) + Ac}\right] - \frac{E(m_2 + E)}{h(m_2 + E) - c}. \tag{5.1}$$

There are two possible cases for MSTY, which we illustrate with examples:

(i) MSTY exists when both species can continue to survive. Take the parameter values A=0.001, $m_1 = 0.15$, $m_2 = 0.25$, h=4.5, c=13. The simulations of changes of yield and equilibrium values with varying effort is shown in Figure 9. It can be seen that when the yield function reaches its maximum value, the prey and predator of the system can coexist, and at this point, $S^* = (0.1531, 0.3504)$, $(E^*, G^*) = (0.5123, 0.2527)$. Further, $\text{Tr}[J_{S^*}] = -0.0185 < 0$, which means the interior equilibrium is stable. Therefore, the system can produce MSTY. From the simulation, we find that the number of prey and predator is monotonous with the harvesting effort.

(ii) There is no MSTY. Take the parameter values A=0.005, $m_1 = 0.125$, $m_2 = 0.4$, h=5, c=7. From Figure 9, we get that when yield reaches its maximum, predator species go to extinction. This is the harvesting of a single species. When the human harvesting of predators gradually increased, the number of predators gradually decreased, and eventually led to the extinction of the predator population.
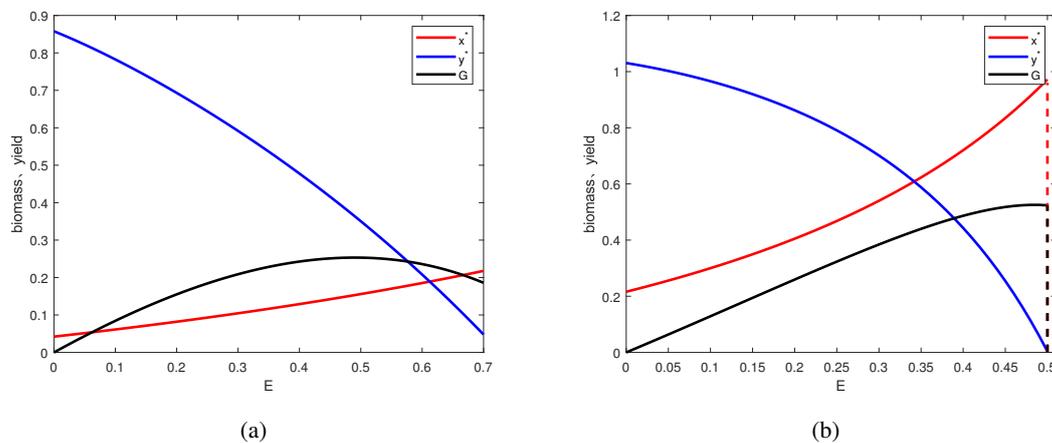

Figure 9. Changes of yield, equilibrium value x^* and y^* with varying effort. (a) Predators and prey coexist, and MSTY exists. (b) Predators go extinct, and MSTY does not exists.

Next, we examine the influence of each parameter change on the system yield $Y(E_1, E_2)$. Model simulations before parameter manipulations are shown in the black line for comparison. When a particular parameter increases by 20%, the yield changes are marked with orange lines, and vice versa with pink lines. In the process of controlling variables, the parameters are given as

$$m_1 = 0.1, m_2 = 0.2, h = 4, c = 4.8, A = 0.04, E_1 = 0.3, E_2 = 0.6. \tag{5.2}$$

By changing the parameters in the yield function, the following radar map of the yield change is obtained. (see Figure 10)

From the simulations, we can observe that when each variable is increased by 20%, the yield will drop to varying degrees, indicating that excessive population harvesting will reduce the population number and economic benefits. Meanwhile, when it is decreased by 20%, the yield will have a different performance. For example, when E_1 decreases by 20%, the yield increases. Therefore, making sustainable yield larger is to achieve the maximum economic benefits to ensure sustainable development rather than blindly improving benefits through a large amount of fishing.
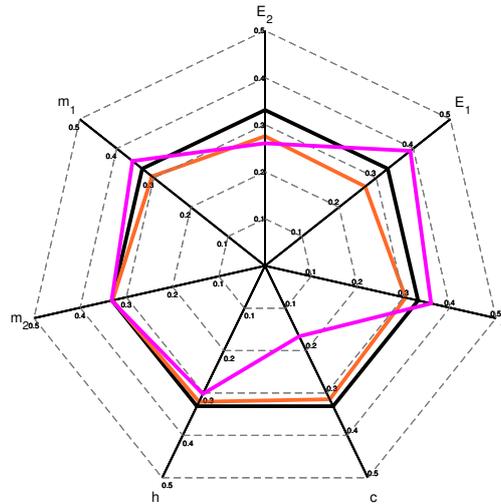
Figure 10. The effect of each parameter on the yield function $Y(E_1, E_2)$.

Next, we examine whether the system exhibits MSY using the methods described in the paper [41]. First, we consider harvesting only the prey, and system (1.3) becomes

$$
\begin{cases}
\dfrac{\mathrm{d}x}{\mathrm{d}t} = x\left(\dfrac{x}{A+x} - m_1 - x - \dfrac{y}{1+hx} - E_1\right), \\
\dfrac{\mathrm{d}y}{\mathrm{d}t} = y\left(\dfrac{cx}{1+hx} - m_2\right).
\end{cases}
\tag{5.3}
$$

The system has the coexisting equilibrium point $S_{E_1}(x_{E_1}, y_{E_1})$, where

$$
x_{E_1} = \frac{m_2}{c - m_2 h} \text{ and } y_{E_1} = \left(\frac{x_{E_1}}{A + x_{E_1}} - m_1 - x_{E_1} - E_1\right)(1 + hx_{E_1}).
$$

The yield at S_{E_1} is $Y_{E_1} = m_2 E_1 / (c - hm_2)$. Clearly, as the harvesting effort intensifies, the equilibrium prey biomass remains constant, while the predator biomass declines. In this scenario, the yield increases with effort and exhibits no maximum point. Consequently, when the effort surpasses a critical threshold, the predator species faces extinction. Therefore, pursuing prey species harvesting at the maximum level is not a sustainable fishing strategy, implying that MSY cannot be attained.

Then, we consider harvesting only the predator, and system (1.3) becomes

$$
\begin{cases}
\dfrac{\mathrm{d}x}{\mathrm{d}t} = x\left(\dfrac{x}{A+x} - m_1 - x - \dfrac{y}{1+hx}\right), \\
\dfrac{\mathrm{d}y}{\mathrm{d}t} = y\left(\dfrac{cx}{1+hx} - m_2 - E_2\right),
\end{cases}
\tag{5.4}
$$

At this time, the coexisting equilibrium point is $S_{E_2}(x_{E_2}, y_{E_2})$, where

$$
x_{E_2} = \frac{m_2 + E_2}{c - m_2 h - E_2 h}, y_{E_2} = \left(\frac{x_{E_2}}{A + x_{E_2}} - m_1 - x_{E_2}\right)(1 + hx_{E_2}),
$$

and the yield from the predator species is

$$Y = -E_2(1 + hx_{E_2})\left(m_1 + x_{E_2} - \frac{m_2 + E_2}{m_2 + E_2 + Ac - Ahm_2 - AhE_2}\right).$$

We use numerical simulations to find MSY. Take the parameter values A=0.003, $m_1 = 0.25$, $m_2 = 0.55$, h=3, c=7.7. The coexisting equilibrium of the system becomes (0.6538,0.2735). The simulations of changes of yield and equilibrium values with varying effort are shown in Figure 11(a).
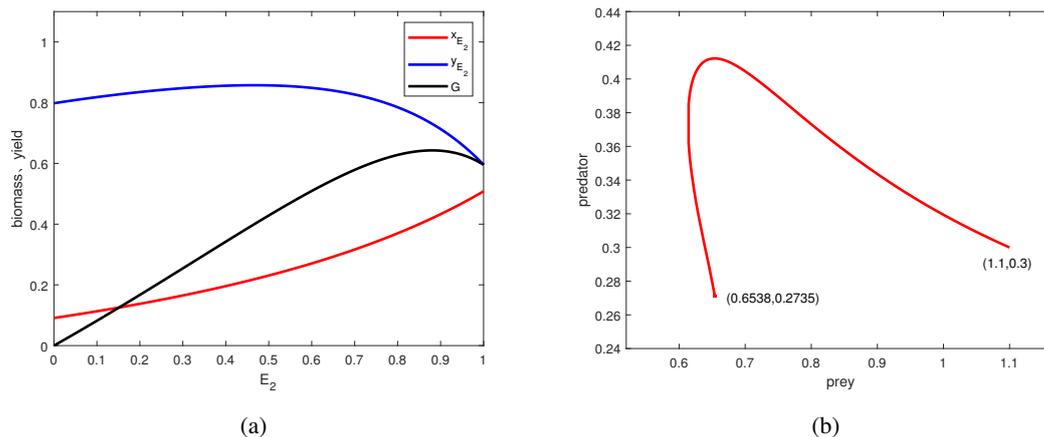

(a)   (b)

Figure 11. (a) Variation of predator biomass and yield with respect to effort. MSY exists at the equilibrium corresponding to the system (5.4). (b) Stability when fishing only for predators.

Therefore, MSY exists when the predator species is harvested. It can be verified that, in this scenario, the coexistence equilibrium point of the system is stable, allowing both species to persist continuously (see Figure 11(b)).

5.2. Optimal harvesting problem

We will discuss the optimal harvesting strategy of the system (1.3). E_1 and E_2 are selected as control variables, and then the control system is as follows:

$$\begin{cases} \dfrac{dx}{dt} = x\left(\dfrac{x}{A + x} - m_1 - x - \dfrac{y}{1 + hx}\right) - E_1 x, \\ \dfrac{dy}{dt} = y\left(\dfrac{cx}{1 + hx} - m_2\right) - E_2 y, \end{cases} \tag{5.5}$$

where $E_i(t)$ $(i = 1, 2)$ are the harvesting efforts of the prey and predator, respectively, which satisfy

$$U = \{(E_1, E_2) \in L^1[0, t_f] \times L^1[0, t_f] | \alpha_1 \le E_1 \le \beta_1, \alpha_2 \le E_2 \le \beta_2\},$$

where α_i, β_i $(i = 1, 2)$ are positive constants. The objective function is given by

$$J = \int_0^{t_f} e^{-\delta t}[(p_1 x - c_1)E_1 + (p_2 y - c_2)E_2]dt,$$

where δ is the continuous annual discount rate. p_1 and p_2 represent the selling prices of the two populations, respectively. c_1 and c_2 represent the fishing costs of the two populations, respectively.

On the premise of ensuring the sustainable development of the system population, the control E_i ($i = 1, 2$) is in U, so that the solution of the system through the initial value (x_0, y_0) makes the performance index J reach the maximum value, that is, the optimal control ($E_1^{\text{opt}}, E_2^{\text{opt}}$) satisfies

$$\max_U J(E_1, E_2) = J_{\text{opt}}(E_1^{\text{opt}}, E_2^{\text{opt}}).$$

We use the maximum principle to get the optimal solution, and the Hamiltonian function H is

$$H = \quad \mathrm{e}^{-\delta t}[(p_1 x - c_1)E_1 + (p_2 y - c_2)E_2] + \lambda_1\left[x\left(\frac{x}{A + x} - m_1 - x - \frac{y}{1 + hx} - E_1\right)\right]$$
$$+ \lambda_2\left[y\left(\frac{cx}{1 + hx} - m_2 - E_2\right)\right],$$

where $\lambda_i(t)$ (i=1,2) are adjoint variables, related to x and y respectively, which can be determined by the following conditions

$$\frac{\mathrm{d}\lambda_1}{\mathrm{d}t} = -\frac{\partial H}{\partial x}, \frac{\mathrm{d}\lambda_2}{\mathrm{d}t} = -\frac{\partial H}{\partial y},$$

and satisfy the transversal conditions

$$\lambda_i(t_f) = 0, i = 1, 2.$$

Then, we can calculate that

$$\begin{cases} \dfrac{\mathrm{d}\lambda_1}{\mathrm{d}t} = -\mathrm{e}^{-\delta t}p_1 E_1 - \lambda_1\left[\dfrac{x^2 + 2Ax}{(A + x)^2} - m_1 - 2x - \dfrac{y}{(1 + hx)^2} - E_1\right] - \lambda_2\dfrac{cy}{1 + hx}, \\ \dfrac{\mathrm{d}\lambda_2}{\mathrm{d}t} = -\mathrm{e}^{-\delta t}p_2 E_2 - \lambda_1\dfrac{x}{1 + hx} - \lambda_2\left(\dfrac{cx}{1 + hx} - m_2 - E_2\right). \end{cases} \quad (5.6)$$

Meanwhile, we have

$$\begin{cases} \dfrac{\partial H}{\partial E_1} = \mathrm{e}^{-\delta t}(p_1 x - c_1) - \lambda_2 x \triangleq \delta_1(t), \\ \dfrac{\partial H}{\partial E_2} = \mathrm{e}^{-\delta t}(p_2 x - c_2) - \lambda_2 y \triangleq \delta_2(t), \end{cases}$$

with control $E_i^b(t)$ ($i = 1, 2$) satisfying

$$E_i^b(t) = \begin{cases} \alpha_i, \delta_i(t) < 0, \\ \beta_i, \delta_i(t) > 0. \end{cases}$$

The control that depends on the switch function $\delta_i(t)$ ($i = 1, 2$) to switch between the minimum and maximum values is a Bang-Bang control [42]. However, when $\delta_i(t) = 0$ ($i = 1, 2$), the Hamiltonian function H does not depend on the control variable $E_i(t)$ ($i = 1, 2$), so the optimal control cannot be determined, and therefore a singular case exists. If condition $\alpha_i < E_i^s < \beta_i$ ($i = 1, 2$) is satisfied, the optimal harvesting strategy is as follows

$$E_i^{\text{opt}}(t) = \begin{cases} E_i^b, \delta_i(t) \neq 0, \\ E_i^s, \delta_i(t) = 0. \end{cases}$$

Singular control occurs at $\sigma_i(t) = 0(i = 1, 2)$, that is

$$\begin{cases} \lambda_1 = e^{-\delta t}\left(p_1 - \dfrac{c_1}{x}\right), \\ \lambda_2 = e^{-\delta t}\left(p_2 - \dfrac{c_2}{y}\right). \end{cases} \tag{5.7}$$

It can be obtained from the above equation

$$\begin{cases} \dfrac{d\lambda_1}{dt} = -\delta e^{-\delta t}\left(p_1 - \dfrac{c_1}{x}\right) + \dfrac{c_1 e^{-\delta t}}{x}\left(\dfrac{x}{A+x} - m_1 - x - \dfrac{y}{1+hx} - E_1\right), \\ \dfrac{d\lambda_2}{dt} = -\delta e^{-\delta t}\left(p_2 - \dfrac{c_2}{y}\right) + \dfrac{c_2 e^{-\delta t}}{y}\left(\dfrac{cx}{1+hx} - m_2 - E_2\right). \end{cases} \tag{5.8}$$

Further, we need to consider the following equation

$$\begin{cases} \left(\dfrac{c_1}{x} - p_1\right)\dfrac{x}{1+hx} - p_2\left(\dfrac{cx}{1+hx} - m_2\right) + \delta\left(p_2 - \dfrac{c_2}{y}\right) = 0, \\ \left(\dfrac{c_1}{x} - p_1\right)\left[\dfrac{x^2 + 2Ax}{(A+x)^2} - x - \dfrac{y}{(1+hx)^2} - \delta\right] - \left(p_2 - \dfrac{c_2}{y}\right)\dfrac{cy}{1+hx} - \dfrac{c_1}{x}\left(\dfrac{x}{A+x} - \dfrac{y}{1+hx}\right) = 0. \end{cases} \tag{5.9}$$

Then, we can get the singular solution (x^s, y^s) from (5.9), which is the optimal equilibrium state of the system, also denoted as (x^{opt}, y^{opt}) [43, 44]. The singular control is

$$\begin{cases} E_1^s = \dfrac{x^s}{A+x^s} - m_1 - x^s - \dfrac{y^s}{1+hx^s}, \\ E_2^s = \dfrac{cx^s}{1+hx^s} - m_2. \end{cases}$$

Before solving the optimal control problem of the system (5.5), let us discuss the following problem first. In order to make the system reach the optimal equilibrium state as soon as possible, we give the following two schemes for comparison.

(i) Plan 1: We adopt the method of combining Bang-Bang control and singular control, and the control scheme is shown as follows

$$E_i^b(t) = \begin{cases} E_i^b, 0 < t < T^{opt}, \\ E_i^s, t > T^{opt}. \end{cases}$$

where T^{opt} represents the time to reach the optimal equilibrium state.

(ii) Plan 2: The system is always harvested using singular control (E_1^s, E_2^s).

First we select the appropriate parameters

$$A = 0.001, m_1 = 0.15, m_2 = 0.25, h = 8, c = 2.4, d = 0.03, p_1 = 20, p_2 = 25, c_1 = 14, c_2 = 16. \tag{5.10}$$

Then we give the domain of control according to the existence and stability of the interior equilibrium point (S^*)

$$U = \{(E_1, E_2)|0 \le E_1 \le 0.25, 0 \le E_2 \le 0.5\}. \tag{5.11}$$

The optimal equilibrium state is $(x^{\text{opt}}, y^{\text{opt}}) = (0.52, 0.21)$, the singular control is $(E_1^s, E_2^s) = (0.0879, 0.0061)$. The optimal yield is 0.047. We choose $t = 10$ as the time period, and find that Plan 1 only needs the maximum harvesting intensity in a short period of time, and will be transformed into the optimal harvesting intensity. Plan 2 always maintains the optimal harvesting intensity. Figure 12 shows the effect of Plans 1 and 2.
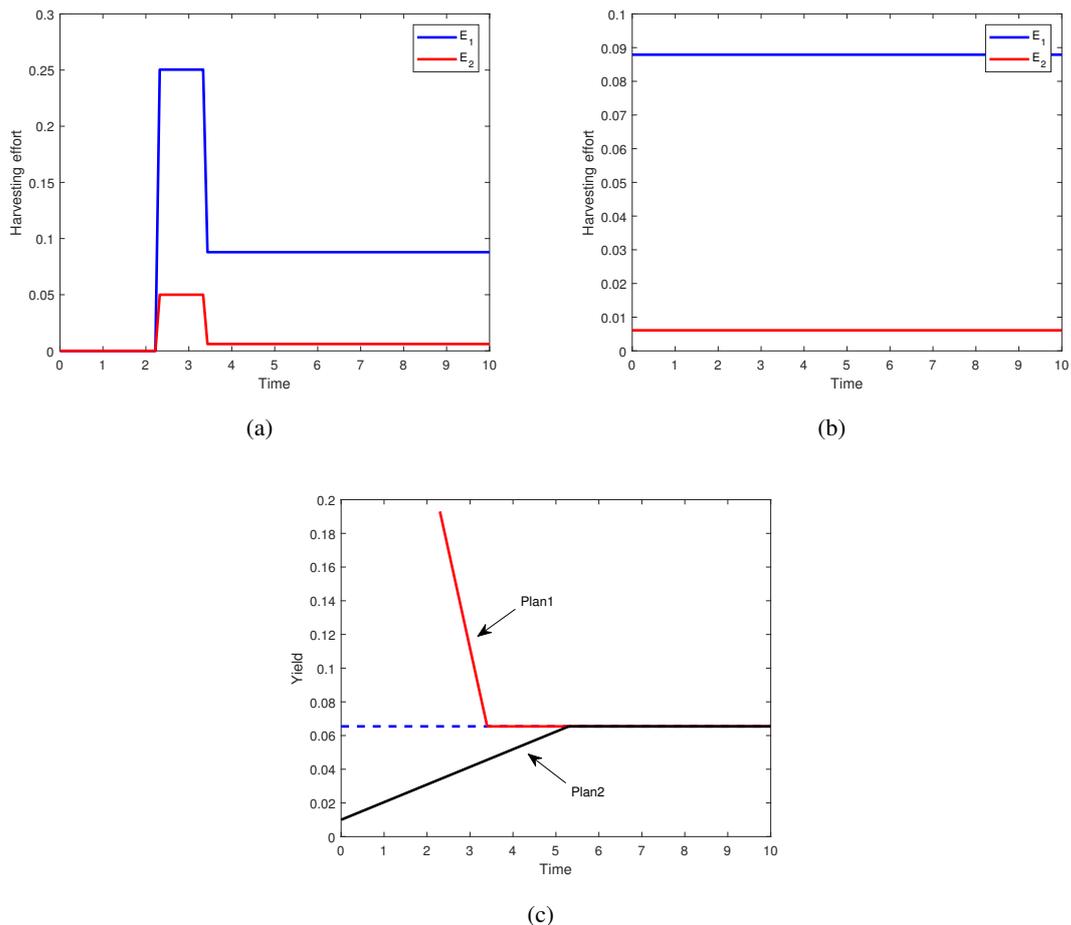

(a)

(b)

(c)

Figure 12. (a) Plan 1. (b) Plan 2. (c) Control effect of Plan 1 and Plan 2.

We can obviously find that Plan 1 takes less time to reach the optimal equilibrium state than Plan 2. Therefore, Plan 1 is the best scheme to control the equilibrium state.

The impact of human harvesting on economic benefits is profound. People aim to maximize the species harvesting through rational strategies to optimize economic gains. In predator-prey systems, preserving population equilibrium and ensuring sustainable resource utilization are of utmost importance. Overfishing or irrational harvesting practices can deplete prey populations, disrupt predator-prey dynamics and lead to ecosystem collapse. Hence, it is imperative to formulate relevant optimal control problems that can provide a scientific basis for real-world scenarios. In the following,

we address the following optimal control problems, denoted as (Q1) and (Q2):

$$\text{(Q1)} \quad \min_{E_1, E_2 \in U} J_1 = \int_0^{t_f} -e^{-\delta t}[(p_1 x - c_1)E_1 + (p_2 y - c_2)E_2]dt,$$

$$\frac{dx}{dt} = x\left(\frac{x}{A+x} - m_1 - x - \frac{y}{1+hx}\right) - E_1 x, \, x(0) = x_0,$$

$$\frac{dy}{dt} = y\left(\frac{cx}{1+hx} - m_2\right) - E_2 y, \, y(0) = y_0,$$

$$\alpha_1 \leq E_1 \leq \beta_1, \alpha_2 \leq E_2 \leq \beta_2.$$

$$\text{(Q2)} \quad \min_{E_1, E_2 \in U} J_2 = \int_0^{t_f} -e^{-\delta t}[(p_1 x - c_1)E_1 + (p_2 y - c_2)E_2]dt,$$

$$\frac{dx}{dt} = x\left(\frac{x}{A+x} - m_1 - x - \frac{y}{1+hx}\right) - E_1 x, \, x(0) = x_0,$$

$$\frac{dy}{dt} = y\left(\frac{cx}{1+hx} - m_2\right) - E_2 y, \, y(0) = y_0,$$

$$x(t_f) = x^{\text{opt}}, y(t_f) = y^{\text{opt}},$$

$$\alpha_1 \leq E_1 \leq \beta_1, \alpha_2 \leq E_2 \leq \beta_2.$$

We use the method of control parametrization to solve the optimal control problem (Q1) and (Q2) with the help of the MISER 3 toolbox of MATLAB. The results are shown in Figure 13.
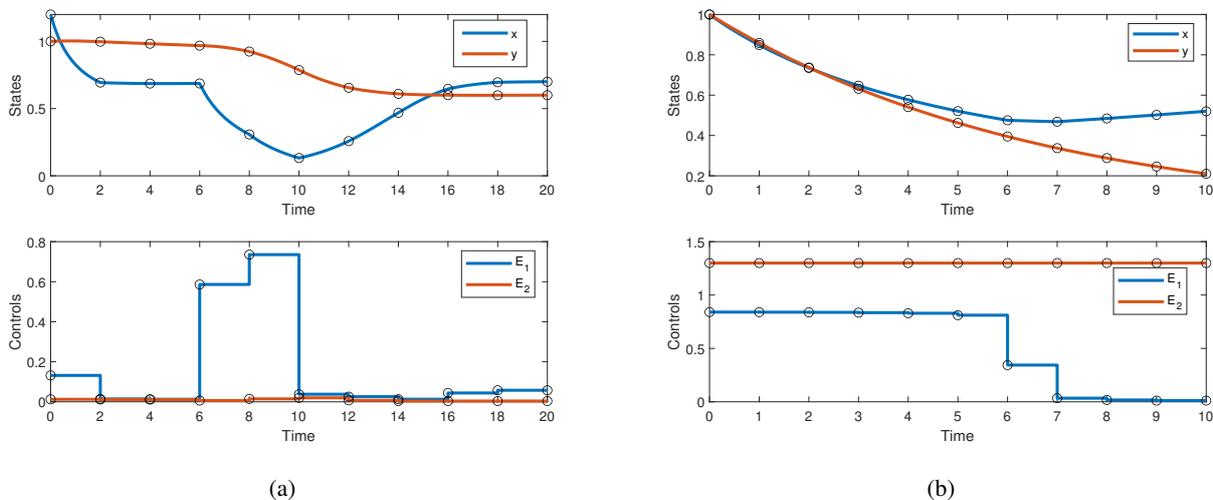

(a)   (b)

Figure 13. (a) The optimal control and state functions of problem (Q1). (b) The optimal control and state functions of problem (Q2). Relevant data sets are shown in (5.10).

For problem (Q1), we choose a final time t_f of 20, initial value (x_0, y_0) of $(1.2, 1)$ and control constraints U of (5.11). Then, we get $J_{\max} = 14.926$. In this problem, we want to find a harvesting strategy that maximizes the amount of prey harvested while minimizing the cost of harvesting to achieve maximum economic profit.

For problem (Q2), we choose a final time t_f of 10, initial value (x_0, y_0) of $(1,1)$ and control constraints U of (5.11). Then, we get $J_{\max} = 0.25$. By solving this optimization problem, we can find the best harvesting strategy to optimize the system and maximize the economic benefit.

These two issues highlight the important role and impact of human harvesting in predator-prey systems and raise the challenge of balancing economic efficiency with sustainability.

6. Conclusions

In this paper, with the Allee effect and harvesting effort at the center, the dynamics of the predator-prey system are researched. We verify that the solutions of system (1.3) are positive and uniformly bounded (see Theorem 1). The local stabilities of the equilibrium points of (1.3) have been investigated. The conditions for the Hopf bifurcation in system (1.3) have been discussed (see Theorem 5). We verify the results by numerical simulations.

Further, we give a simple comparison of systems with and without harvesting effort (system (1.1) and system (1.3)) to study the effects of harvesting terms. In addition, we find that the sensitivity of the predator population to different parameters is different, especially when the predator population is harvested, and it is susceptible to the influence of c (see Figure 6). Both theoretical and numerical results show that, in the predator-prey systems (1.3), the harvesting effort weakens the Allee effect and makes it easier for the system to reach a coexistence state. However, the coexistence of prey and predator also depends on their initial population densities within the prey population, which are influenced by the harvesting effort. We can determine whether the system is stable or oscillating periodically by controlling the threshold of the harvesting effort and the initial value of the system (see Figures 3–5).

Through our study of the Allee effect, we have found that the strength of the Allee effect is determined by the parameter A. When the Allee effect is robust, populations tend towards extinction, resulting in a reduced stable range for both prey and predators. Interestingly, substantial disparities in the initial populations of predators and prey can trigger dynamical changes in the sizes of both populations over time.

When it comes to MSY and MSTY, we explore four distinct scenarios: different harvesting efforts, uniform harvesting efforts, exclusive prey harvesting and exclusive predator harvesting. In our investigations, we identify MSTY in the case of uniform harvesting efforts, which maintained system population stability. Furthermore, we determine that MSY could be achieved through predator harvesting, also resulting in a stable system population.

It is a combination of Bang-Bang control and singular control to achieve the optimal equilibrium state (see Figure 12). In addition, we establish objective optimization, and problem (Q1) finds the best harvesting strategy to maximize economic benefits while problem (Q2) finds the best harvesting strategy under the condition that the termination state is the optimal equilibrium state and the economic benefits are maximized, which has guiding significance for realistic harvesting. These results are shown in Figure 13.

In natural ecosystems, populations can be vulnerable to substantial Allee effects, which may drive species towards extinction. Human intervention through harvesting can mitigate these effects, increasing the likelihood of population coexistence. This approach plays a crucial role in maintaining stable population densities over the long term and reducing the risk of extinction. In the realm of fisheries, responsible fishing practices play a crucial role in promoting sustainable stock growth and fostering the development of the fishing industry.

Use of AI tools declaration

The authors declare they have not used Artificial Intelligence (AI) tools in the creation of this article.

Acknowledgments

Conflict of interest

All authors declare no conflicts of interest in this paper.

References

1. R. J. Han, L. N. Guin, B. X. Dai, Consequences of refuge and diffusion in a spatiotemporal predator-prey model, *Nonlinear Anal. Real*, **60** (2021), 103311. https://doi.org/10.1016/j.nonrwa.2021.103311

2. L. N. Guin, P. K. Mandal, Effect of prey refuge on spatiotemporal dynamics of the reaction-diffusion system, *Comput. Math. Appl.*, **68** (2014), 1325–1340. https://doi.org/10.1016/j.camwa.2014.08.025

3. X. X. Liu, Q. D. Huang, Dynamics of a predator-prey system with inducible defense and disease in the prey, *Nonlinear Anal. Real*, **71** (2023), 103802. https://doi.org/10.1016/j.nonrwa.2022.103802

4. D. M. Johnson, A. M. Liebhold, P. C. Tobin, O. N. Bjørnstad, Allee effects and pulsed invasion by the gypsy moth, *Nature*, **444** (2006), 361–363. https://doi.org/10.1038/nature05242

5. L. Hammann, B. Silliman, B. Blasius, Optimal planting distance in a simple model of habitat restoration with an Allee effect, *Front. Mar. Sci.*, **7** (2021), 610412. https://doi.org/10.3389/fmars.2020.610412

6. R. A. Morris, A. Hernández-Flores, F. Aranceta-Garza, A. Cuevas-Jiménez, K. Kitson-Walters, Allee effect considerations to support the spatial management of a sedentary marine species: The queen conch (Aliger gigas) on the Pedro Bank, Jamaica, *Mar. Freshwater Res.*, **74** (2023), 375–386. https://doi.org/10.1071/MF22140

7. D. W. Morris, Measuring the Allee effect: positive density dependence in small mammals, *Ecology*, **83** (2002), 14–20. https://doi.org/10.1890/0012-9658(2002)083[0014:MTAEPD]2.0.CO;2

8. G. Mandal, S. Das, L. N. Guin, S. Chakravarty, Dynamic response of a system of interactive species influenced by fear and Allee consequences, *Eur. Phys. J. Plus*, **138** (2023), 661. https://doi.org/10.1140/epjp/s13360-023-04246-0

9. J. Gascoigne, L. Berec, S. Gregory, F. Courchamp, Dangerously few liaisons: A review of mate-finding Allee effects, *Popul. Ecol.*, **51** (2009), 355–372. https://doi.org/10.1007/s10144-009-0146-4

10. D. Sen, S. Ghorai, S. Sharma, M. Banerjee, Allee effect in prey's growth reduces the dynamical complexity in prey-predator model with generalist predator, *Appl. Math. Model.*, **91** (2021), 768–790. https://doi.org/10.1016/j.apm.2020.09.046

11. J. P. Tripathi, P. S. Mandal, A. Poonia, V. P. Bajiya, A widespread interaction between generalist and specialist enemies: The role of intraguild predation and Allee effect, *Appl. Math. Model.*, **89** (2021), 105–135. https://doi.org/10.1016/j.apm.2020.06.074

12. D. W. Goodsman, M. A. Lewis, The minimum founding population in dispersing organisms subject to strong Allee effects, *Methods Ecol. Evol.*, **7** (2016), 1100–1109. https://doi.org/10.1111/2041-210X.12573

13. C. Zhang, X. Y. Li, Dynamics of a discrete Leslie-Gower model with harvesting and Holling-II functional response, *Mathematics*, **11** (2023), 3303. https://doi.org/10.3390/math11153303

14. Z. W. Xiao, X. D. Xie, Y. L. Xue, Stability and bifurcation in a Holling type II predator-prey model with Allee effect and time delay, *Adv. Differ. Equ.*, **2018** (2018), 288. https://doi.org/10.1186/s13662-018-1742-4

15. W. X. Wang, Y. B. Zhang, C. Z Liu, Analysis of a discrete-time predator prey system with Allee effect, *Ecol. Complex.*, **8** (2011), 81–85. https://doi.org/10.1016/j.ecocom.2010.04.005

16. X. Q. Wang, Y. L. Cai, H. H. Ma, Dynamics of a diffusive predator-prey model with Allee effect on predator, *Discrete Dyn. Nat. Soc.*, **2013** (2013), 984960. https://doi.org/10.1155/2013/984960

17. R. D. Parshad, E. Quansah, K. Black, R. K. Upadhyay, S. K. Tiwari, N. Kumari, Long time dynamics of a three-species food chain model with Allee effect in the top predator, *Comput. Math. Appl.*, **71** (2016), 503–528. https://doi.org/10.1016/j.camwa.2015.12.015

18. E. González-Olivares, H. Meneses-Alcay, B. González-Yañez, J. Mena-Lorca, A. Rojas-Palma, R. Ramos-Jiliberto, Multiple stability and uniqueness of the limit cycle in a Gause-type predator-prey model considering the Allee effect on prey, *Nonlinear Anal. Real*, **12** (2011), 2931–2942. https://doi.org/10.1016/j.nonrwa.2011.04.003

19. H. Y. Liu, H. G. Yu, C. J. Dai, Z. L. Ma, Q. Wang, M. Zhao, Dynamical analysis of an aquatic amensalism model with non-selective harvesting and Allee effect, *Math. Biosci. Eng.*, **18** (2021), 8857–8882. https://doi.org/10.3934/mbe.2021437

20. J. F. Wang, J. P. Shi, J. J. Wei, Dynamics and pattern formation in a diffusive predator-prey system with strong Allee effect in prey, *J. Differ. Equations*, **251** (2021), 1276–1304. https://doi.org/10.1016/j.jde.2011.03.004

21. M. Y. Hamada, T. El-Azab, H. El-Metwally, Allee effect in a Ricker type predator-prey model, *J. Math. Comput. Sci-JM.*, **29** (2023), 239–251. https://doi.org/10.22436/jmcs.029.03.03

22. S. Rana, S. Bhattacharya, S. Samanta, Spatiotemporal dynamics of Leslie-Gower predator-prey model with Allee effect on both populations, *Math. Comput. Simulat.*, **200** (2022), 32–49. https://doi.org/10.1016/j.matcom.2022.04.011

23. J. Zu, M. Mimura, The impact of Allee effect on a predator-prey system with Holling type II functional response, *Appl. Math. Comput.*, **217** (2010), 3542–3556. https://doi.org/10.1016/j.amc.2010.09.029

24. J. A. Dunne, R. J. Williams, N. D. Martinez, Network structure and biodiversity loss in food webs: Robustness increases with connectance, *Ecol. Lett.*, **5** (2002), 558–567. https://doi.org/10.1046/j.1461-0248.2002.00354.x

25. B. Ghosh, T. K. Kar, Sustainable use of prey species in a prey-predator system: Jointly determined ecological thresholds and economic trade-offs, *Ecol. Model.*, **272** (2014), 49–58. https://doi.org/10.1016/j.ecolmodel.2013.09.013

26. X. X. Liu, Q. D. Huang, Analysis of optimal harvesting of a predator-prey model with Holling type IV functional response, *Ecol. Complex.*, **42** (2020), 100816. https://doi.org/10.1016/j.ecocom.2020.100816

27. X. X. Liu, Q. D. Huang, Dynamics and optimal control of a Monod-Haldane predator-prey system with mixed harvesting, *Int. J. Bifurcat. Chaos*, **30** (2020), 2050243. https://doi.org/10.1142/S0218127420502430

28. T. Das, R. N. Mukherjee, K. S. Chaudhuri, Harvesting of a prey-predator fishery in the presence of toxicity, *Appl. Math. Model.*, **33** (2009), 2282–2292. https://doi.org/10.1016/j.apm.2008.06.008

29. S. G. Mortoja, P. Panja, S. K. Mondal, Stability analysis of plankton-fish dynamics with cannibalism effect and proportionate harvesting on fish, *Mathematics*, **11** (2023), 3011. https://doi.org/10.3390/math11133011

30. C. J. Wei, L. S. Chen, Periodic solution and heteroclinic bifurcation in a predator-prey system with Allee effect and impulsive harvesting, *Nonlinear Dyn.*, **76** (2014), 1109–1117. https://doi.org/10.1007/s11071-013-1194-z

31. Z. C. Shang, Y. H. Qiao, Multiple bifurcations in a predator-prey system of modified Holling and Leslie type with double Allee effect and nonlinear harvesting, *Math. Comput. Simulat.*, **205** (2023), 745–764. https://doi.org/10.1016/j.matcom.2022.10.028

32. D. Y. Wu, H. Y. Zhao, Y. Yuan, Complex dynamics of a diffusive predator-prey model with strong Allee effect and threshold harvesting, *J. Math. Anal. Appl.*, **469** (2019), 982–1014. https://doi.org/10.1016/j.jmaa.2018.09.047

33. S. S. Yu, J. Liu, X. J. Lin, Multiple positive periodic solutions of a Gause-type predator-prey model with Allee effect and functional responses, *Aims Math.*, **5** (2020), 6135–6148. https://doi.org/10.3934/math.2020394

34. R. P. Gupta, D. K. Yadav, Role of Allee effect and harvesting of a food-web system in the presence of scavengers, *J. Biol. Syst.*, **30** (2022), 149–181. https://doi.org/10.1142/S021833902250005X

35. B. Barman, B. Ghosh, Dynamics of a spatially coupled model with delayed prey dispersal, *Int. J. Model. Simul.*, **42** (2021), 400–414. https://doi.org/10.1080/02286203.2021.1926048

36. C. Roberts, *Ordinary differential equations: Applications, models, and computing*, New York: Chapman and Hall, 2011. https://doi.org/10.1201/b15111

37. Y. A. Kuznetsov, *Elements of applied bifurcation theory*, New York: Springer, 2004. https://doi.org/10.1007/978-1-4757-3978-7

38. L. Perko, *Differential equations and dynamical systems*, New York: Springer, 1991. https://doi.org/10.1007/978-1-4684-0392-3

39. B. Ghosh, T. K. Kar, T. Legović, Sustainability of exploited ecologically interdependent species, *Popul. Ecol.*, **56** (2014), 527–537. http://doi.org/10.1007/s10144-014-0436-3

40. B. Ghosh, D. Pal, T. Legović, T. K. Kar, Harvesting induced stability and instability in a tri-trophic food chain, *Math. Biosci.*, **304** (2018), 89–99. http://doi.org/10.1016/j.mbs.2018.08.003

41. B. Ghosh, T. K. Kar, T. Legović, Relationship between exploitation, oscillation, MSY and extinction, *Math. Biosci.*, **256** (2014), 1–9. http://doi.org/10.1016/j.mbs.2014.07.005

42. L. S. Pontryagin, *Mathematical theory of optimal processes*, London: Routledge, 1987. https://doi.org/10.1201/9780203749319

43. C. W. Clark, *Mathematical bioeconomics: The optimal management of renewable resources*, 1990.

44. A. Rojas-Palma, E. González-Olivares, Optimal harvesting in a predator-prey model with Allee effect and sigmoid functional response, *Appl. Math. Model.*, **36** (2012), 1864–1874. https://doi.org/10.1016/j.apm.2011.07.081